4-Aminophenol Electrochemical Sensing Through Gas-Phase Mono and Bimetallic Clusters Decorated ZnO Nanorods

Giorgia Fiaschi[1*], Salvatore Cosentino[2], Richa Pandey[1], Salvo Mirabella[3], Vincenzina Strano[3], Luca Maiolo[4], Didier Grandjean[2], Peter Lievens[2], Yosi Shacham-Diamand[1]

[1] Dept. of Phys. Elect. Engineering Faculty, Tel Aviv University, Tel Aviv 69978, Israel

[2] Laboratory of Solid State Physics and Magnetism, KU Leuven, Celestijnenlaan 200D, Leuven, Belgium

[3] MATIS CNR-IMM and Dip. Fisica e Astronomia, Catania University, Via Santa Sofia 64, 95123 Catania, Italy

[4] CNR-IMM, Via del Fosso del Cavaliere 100, 00133 Roma, Italy

giorgia.fiaschi@gmail.com

Abstract

The definition of a simple and reliable method for the detection of 4-aminophenol represents an important issue in chemical and pharmaceutical processes, due to the toxicity of this product in humans. A possible route to solve the problem is related to the implementation of electrochemical biosensors with specific nanostructured materials. Indeed, the performance of an electrochemical biosensor strongly depends on the electrode materials, composition and morphology. In this work, we demonstrate the use of a hybrid approach: metal nanoparticles on semiconductor nanorods as functional material for the 4-aminophenol detection.

In particular, we investigate the role of metal nanoclusters, such as AuxPt1-x (x = 0, 0.5, 1) clusters, on ZnO nanorods to enhance the sensitivity of the device: to finely tune the

composition and the size of the metal nanoclusters we used a Laser Ablation Cluster Beam Deposition setup. We adopt three different electrochemical techniques to analyze the sensor performance with the different nanomaterials: Electrochemical Impedance Spectroscopy, Cyclic Voltammetry and Chronoamperometry. A significant improvement in 4-aminophenol detection was observed respect to the simple ZnO nanostructure. In particular, the AuPt/ZnO electrodes showed an enhanced sensitivity of 14.31 μA/mM cm2 and a limit of detection of 3.6 μM, thus revealing a possible candidate to accomplish a simple and reliable detection for the 4-aminophenol.

Introduction

Paracetamol is a well-known drug, used to treat fever and to relieve mild to moderate pain. Due to the very similar chemical structure of paracetamol with respect to aspirin, this compound activates the same enzyme that synthesizes the prostaglandins [1]. These biomolecules are involved, for example, in the dilation of blood vessels, thus reducing the pain related to headache. Paracetamol is produced in huge quantities and it is commonly synthesized in tablets of 250 or 500 mg per tablet, through the reaction of acetylation of 4-aminophenol (pAP) with acetic anhydride [2]. Therefore, 4-aminophenol is typically the main impurity of paracetamol containing pharmaceuticals, being its primary hydrolytic degradation product. The level of pAP in drugs is limited to 50ppm (limit of detection (LOD) = 2.3 $x10^{-5}$ mol/L) by the European, United States and Chinese Pharmacopoeias authorities [3-5], due to its significant nephrotoxicity and teratogenic effect in humans.

Thus, establishment of a simple and robust method to evaluate the content of pAP in paracetamol is highly desirable. As a result, the number of studies related to this matter has increased in the last few years and many different methods have been proposed for the

detection of pAP. There are optical [6-8], mechanical [9] and electrochemical methods, which are effective due to the electroactivity of the pAP [10-13]. Among all those methods, there are several advantages associated with the electrochemical detection, such as relatively simple miniaturization and integration with very large scale integrated (VLSI) circuits, remarkable sensitivity, low cost and low-power requirement [14-15]. Therefore, electrochemical detection has been proven as the most widely reported method in basic research and the medical field [16]. The choice of material and the rate of charge transfer during the electrochemical reaction is crucial to obtain a high sensitive device in order to achieve the abovementioned LOD. In this paper we present the use of a combination of nanostructures enhancing significantly the electrochemical sensitivity of the working electrode.

We show that nearly mono-dispersed Au_xPt_{1-x} (x = 0, 0.5, 1) clusters deposited on semiconducting nanostructures allow to achieve very efficient electrochemical sensing of 4-aminophenol. Zinc Oxide (ZnO) was chosen as the semiconductor template of the sensor. ZnO is a metal-oxide semiconductor with a wide direct band gap (~3.4eV), high electron mobility and good transparency in the visible region that has been intensively employed in bioelectronics due to its biocompatibility, fast electron transfer rate and high isoelectric point (IEP) of 9.5. Furthermore, ZnO offers good binding chemistry, permitting the immobilization of proteins by electrostatic adsorption in proper buffer solutions [17]. Hence, different biosensors based on ZnO nanomaterials have been developed for the detection of glucose [18-21], tyrosinase [22], uric acid [23]. Moreover, ZnO nanostructures such as nanowires, nanotubes, nanowalls and nanorods can be easily synthesized [24-25]. In this regard, nanostructure morphology is an important parameter, since a larger surface area to volume ratio can efficiently enhance biosensor performance.

As aforementioned, the numerous properties of ZnO nanostructure can be further improved by adding metal nanoparticles at its surface. Metal nanoparticles are able to electrically interface the redox centers in biomolecules with the electrode surface, enhancing the electron transfer efficiency between the electrode and the electrolyte, and thus working as catalysts in the activation of electrochemical reaction [26]. Gold nanoparticles have been intensively applied as the active sites in bio-sensing areas, offering a good choice for achieving high performance sensors. Gold nanoparticles are also used as a suitable platform for functionalization with organic or biological ligands for binding and detection of bio-molecules [29-32]. Other types of metal nanoparticles showing even better performances have been investigated, leading to the utilization of metals such as Pt, known to be an excellent biocompatible catalyst [33-35]. Furthermore, it has been shown that bimetallic catalysts offer new properties, distinct from those of their monometallic counterparts [36-38].

Therefore, the choice of metal, loading, matrix, particle size and purity play all a significant role in the sensing performances [27]. However, a fine control of all these properties remains very challenging. The option we present here is to use nearly mono-dispersed nanoclusters synthesized by Cluster Beam Deposition (CBD). Indeed, the use of a CBD for the production of mono and bimetallic nanoclusters (NCs) offers a unique deposition method allowing precise control of clusters density, size and stoichiometry where alloy nanoparticles are needed [28].

This approach allows to investigate more precisely the role of metal nanoparticles and its composition on the sensing response of biosensors based of metal-oxides, ruling out effects due to poly-dispersion and inhomogeneity of clusters. Hence, besides the studies of monometallic Au and Pt clusters, we investigate the response of a bimetallic AuPt clusters deposited on ZnO nanorods towards the detection of 4-aminophenol. This approach provides an effective strategy to further improve the performance of electrochemical biosensors by the

high charge transfer of Pt properties and retaining, at the same time, the bio-linking capabilities of the Au.

2. Experimental

2.1. Materials, Chemicals and solutions

All the solutions were prepared by using purified de-ionized water in a MilliQ Millipore system from Billerica, MA, USA, and the pH values of the buffer solutions were determined with a pH analyzer. 4-Aminophenol (pAP) was purchased from Sigma-Aldrich (≥ 98%). The working standard solutions were daily prepared by appropriate dilution of the stock solutions with 0.1 M phosphate buffer solution (PBS) at pH 7.4. The PBS content was: sodium chloride (NaCl) – 0.14M , potassium chloride (KCl) – 0.003M , potassium phosphate, monobasic, anhydrous (KH_2PO_4) – 0.001M , and sodium phosphate, dibasic, di-hydrous (Na_2HPO_4 $2H_2O$) – 0.03M.

2.2. ZnO nanorods fabrication

ZnO nanorods were grown on conducting Indium Tin Oxide (ITO) glass substrate by Chemical Bath Synthesis (CBS). ITO substrates were cleaned in ultrasonic bath with isopropanol for 90'' and RCA-1 bath for 25'. Then, a solution of 5mM Zinc acetate dehydrate in ethanol, was spin-coated (1000 rpm, 60 s) over the substrate and dried on a hot plate at 120°C for 20 minutes in order to form a seed layer composed by ZnO clustered in small islands (2-3 nm average size, and 60nm average separation distance between them).

Then an open beaker was filled with a solution of Zinc nitrate hexahydrate (Sigma-Aldrich purum p.a. crystallized, 99%) and HMTA (Sigma-Aldrich puriss. p.a., Reag. Ph. Eur., 99.5%) with the same concentration (25mM) in deionized (DI) water, well stirred and pre-heated at

90°C. The resulting pH of the solution was 5.7. Consequently, the seeded substrate was vertically immersed in an open beaker for 1 hour at 95°C to guarantee uniform nanorods growth. All samples were rinsed with DI water and dried in N_2 gas.

2.3. Clusters deposition

Au, AuPt and Pt clusters were produced in ultra-high vacuum condition by a CBD and deposited on ZnO nanorods sample. The setup is described in full detail in [13]. Briefly, clusters are produced by pulsed lased ablation of a metal target from two Nd:YAG lasers (Spectra Physics Quanta-Ray INDI 40-10). The energy of the lasers (λ=532 nm, power~ 250 mW) is transferred to the target and causes evaporation of target atoms. Simultaneously, a liquid-N_2 cooled He carrier gas under high pressure is pulsed in the source chamber. This gas is responsible for the clusters aggregation and for the increase of pressure needed to expand the cluster beam supersonically through a nozzle into the vacuum. Finally, the beam of clusters is guided via an extraction chamber to the deposition stage. Laser ablation of different targets allows the production of clusters with different composition by proper tuning of laser power and choice of target material. Here we chose three different targets: Au, Pt and Au 50 at. 50%-Pt (AuPt). The cluster production, e.g. the size distribution, crucially depends on various experimental parameters. In this work the clusters were deposited without being mass or size selected, thus resulting in a homogeneous beam of clusters (~80% neutral, ~10% positively charged, ~10% negatively charged) with an average diameter lower than 3 nm average size. Cluster size distribution was monitored using reflected time-of-flight (RTOF) mass spectrometry, and the resulting mass spectra are shown in the Supplementary Information (Fig. S1).

The quantity of deposited clusters was evaluated during deposition, using a quartz microbalance and checked ex-situ through Rutherford backscattering spectrometry (RBS). All samples were decorated with 5 atomic monolayers (MLs, 1 ML ≈ 1.55×10^{15} atoms), which means that 5ML is the equivalent thickness of metal deposited directly on top of the ZnO nanorods.

2.4. Electrochemical characterization

All the electrochemical measurements were carried out using a Potentiostat/Galvanostat (VSP BioLogic Inc. SP-200), and analyzed with EC-Lab™ software. The electrolyte used was diluted PBS (pH=7.4) (1:10 v/v PBS: H_2O). The system was configured with an Ag/AgCl homemade quasi-reference electrode (RE) and Pt wire as counter electrode (CE). The Ag/AgCl homemade reference electrode stability was tested versus commercial Ag/AgCl (Saturated KCl) electrodes and was found to be stable with very low drift in standard PBS solution. The Working Electrode's surface area was occluded by polystyrene tube (∅ = 6 mm, h = 10 mm, A = 0.282 cm^2) glued to the clean electrode surface. Prior to use, the electrodes were washed with isopropanol and dried with a nitrogen flux.

Electrochemical impedance spectroscopy (EIS) was performed at room temperature first in PBS (0.1 M) and then with the addition of 0.1 mg/ml pAP ml (= 0.0916mM) in the PBS. The results were plotted in the form of Nyquist and Bode plot, with a frequency range of 100 mHz – 500 kHz.

The cyclic voltammetric detection (CV) was studied in a voltage range of -0.5 to 0.5 V with three cycles per each measurement. Chronoamperometry (CA) characterization was performed at an applied voltage of 0.375V, adding at each step 0.01 mg/ml of pAP to the PBS.

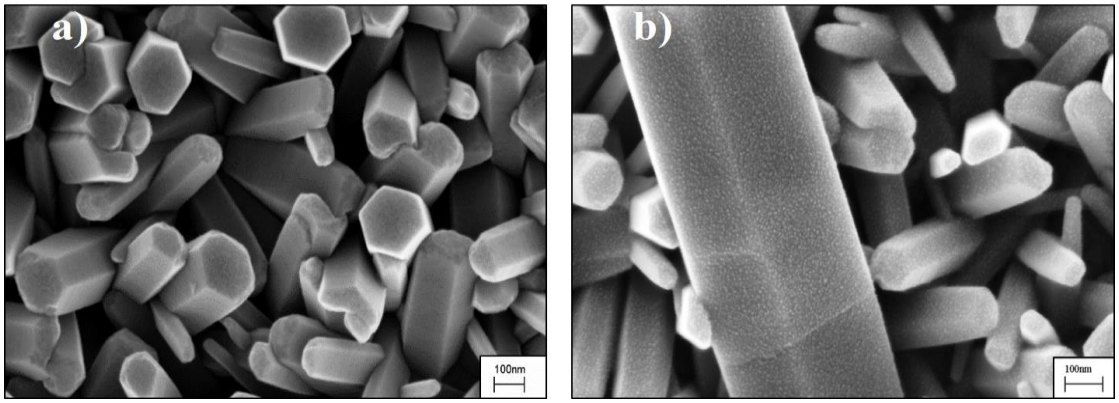

3. Results and discussion

3.1 SEM characterization

Fig.1 – (a) SEM pictures of bare ZnO electrode and (b) after the deposition of 5ML (Mono Layer equivalent) of Au clusters on top. Similar results are observed for Pt or AuPt clusters.

Fig.1 shows typical SEM micrographs of the as prepared ZnO and Au/ZnO modified electrode. ZnO nanorods have an average diameter of 120 nm and a height between 400 and 800 nm and exhibit a random misalignment around the vertical orientation.. The estimated density of the nanorods is about $10^9/cm^2$. After cluster deposition, ZnO nanorods retain their initial features, while the presence of Au clusters, attached onto the electrode surface, is clearly observed. The nanostructured substrate allows a higher surface coverage of the clusters compared to planar surface. By assuming spherical-like and isolated clusters, the average density of clusters deposited on the overall surface area exposed by ZnO nanorods is around 10^{12} clusters/cm^2, which means that the surface of each nanorod is decorated by about 10^3 clusters, thus obtaining a clusters coverage of ~43% of the total area of the nanostructures.

3.2 Electrochemical Impedance Spectroscopy

Electrochemical impedance spectroscopy (EIS) was applied in order to study the interfacial properties of the ZnO and the cluster modified ZnO electrodes in contact with a buffered solution containing the 0.1 mg/ml of the designated product, pAP. This product is typical to many enzyme sensors, especially in whole cell biosensors [39].

Fig.2 exhibits the Nyquist plot of the measured impedance vs. frequency for bare and modified electrodes without and with pAP.

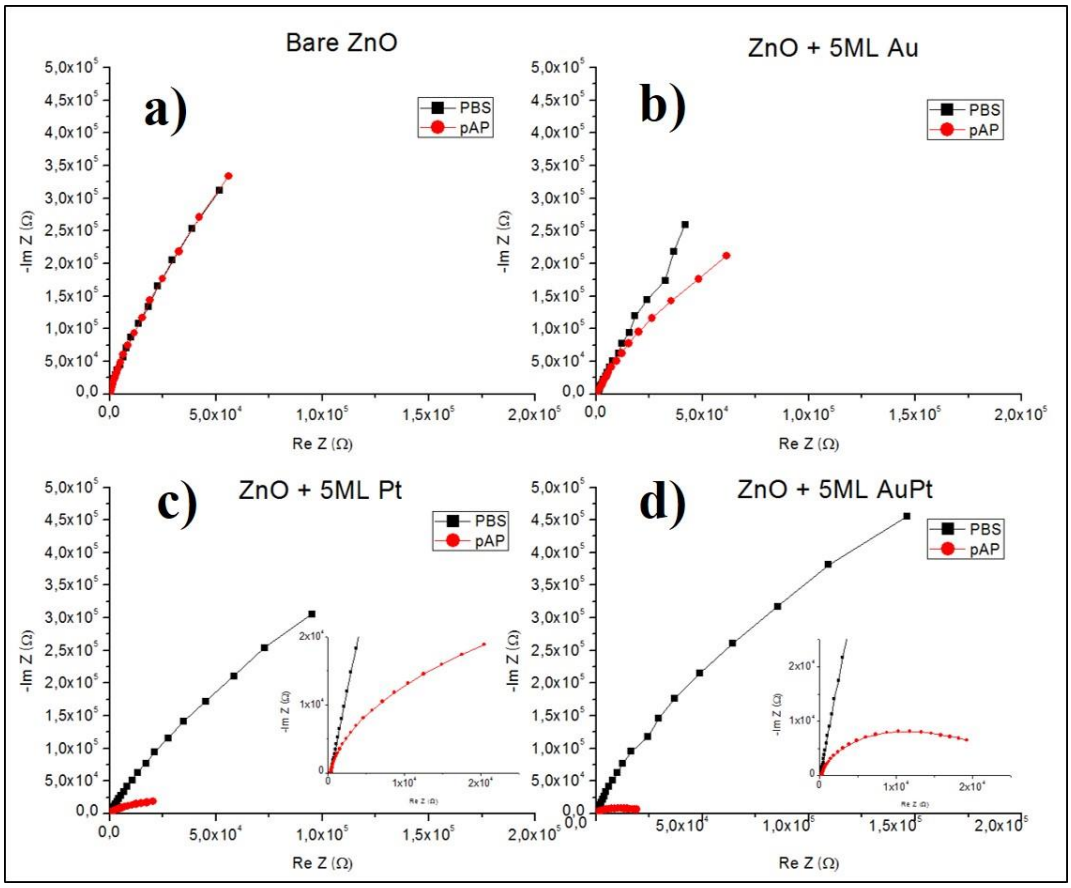

Fig. 2 – Nyquist diagrams recorded in presence of pure PBS (black line) and of the mixture of pAP in PBS (red line) for bare ZnO (a), and nanocluster modified Au/ZnO (b), Pt/ZnO (c) and AuPt/ZnO (d). The injected product solution includes pAP (0.1 mg/ml) in PBS (0.1M). The insets present the enlarged plots for high frequencies.

In the presence of only PBS, the bare ZnO electrode and the Au/ZnO modified electrode show an almost similar Nyquist plot, due to the limited charge transfer with the ions in the buffer solution.

After the pAP injection, no significant changes due to the added Au clusters that can be detected after the addition of the analyte. On the contrary, a very distinct behavior is observed for Pt/ZnO and AuPt/ZnO electrodes in comparison to the bare ZnO electrode. Pt and AuPt clusters significantly reduce the electrode impedance by more than an order of magnitude in the presence of pAP. This effect can be described as a "depressed semicircle" of the Pt and AuPt modified electrodes compared to those of ZnO and the gold modified ZnO nanorods. Generally, the formation of a depressed semicircle at high frequency (visible in the presence of pAP for the Pt/ZnO and the AuPt/ZnO electrodes) indicates a significantly smaller real part of the impedance, which is due to the charge transfer resistance, R_{ct}. The charge transfer resistance depends on the electron-transfer kinetics at the electrode interface [40].

To describe the behavior of the impedance for the various electrodes in presence of pAP we applied the simplest equivalent circuit known in the literature as the Randles model [41]. According to this model, the electrode impedance can be in first approximation modeled as the series of the electrolyte resistance (R_{Ω}), with the parallel between the electron transfer resistance (R_{ct}), the double layer capacitance (C) and the Warburg element (W). The fit and the resulting parameters obtained are given in the Supporting Information (Fig. S2 and Table S1) section.

The pAP molecule is known to undergo oxidation, forming quinoneimine, which can be reduced back to pAP [39]. Due to this reaction, the electrons can be transferred across the interface by overcoming an appropriate activation barrier, which can be in first approximation assessed by looking at the R_{ct} values. The calculated R_{ct} was 252kΩ (bare ZnO), 200kΩ (Au/ZnO), 25kΩ (Pt/ZnO) and 20kΩ (AuPt/ZnO) respectively. These results

indicate that a minimal coverage of Pt and AuPt cluster-based catalysts can efficiently enhance the electron transfer rate by an order of magnitude. The reduction of the R_{ct} values, which is due to the unique properties of Pt, can be associated with the activation energy barrier between the electrode and the solution and the number of conduction band electrons in the electrode. The fact that has a higher work function (in vacuum) than gold (5.65 eV vs. 5.1 eV) might lower the energy barrier for the electron transfer from the metal to the electrolyte. This shift in the Fermi level between Au and Pt is an indication of the better charge separation and more reducing power of the Pt [42] that consequently, is able to provide a good electron exchange with the solution and accelerate the electron transfer kinetics. This is not necessarily the only reason as the electron transfer across the metal/electrolyte barrier depends also on the surface electrical and chemical properties and its interaction with the electrolyte. Note that the electron transfer from the electrode in our case is probably a two-step process from the ZnO to the clusters and from the clusters to the electrolyte.

Nevertheless, the current flowing at the interface always contains non-Faradaic components resulting from the charging of the double layer capacitor C_{dl}. The double layer capacitance has two parallel components, one due to the semiconductor/electrolyte interface ($C_{dl.SC}$) and one due to the cluster/electrolyte interface ($C_{dl,C}$). In our case $C_{dl.SC} >> C_{dl,C}$ since (a) the semiconductor/electrolyte interface has an additional capacitance due to the surface states of ZnO and (b) the metal nanoclusters occupy less than half (~43%) of the overall electrode area. Therefore, the contribution of the metal clusters to the overall double layer capacitance is negligible [43].

3.3 Cyclic Voltammetry

The aforementioned two-electron redox reaction of pAP on the electrode surface generates a current, thus producing, in the presence of suitable supporting electrolytes quasi-reversible redox peaks, spaced by about a few hundreds of mV at scan rates on the order of 50 mV/s [12]. Generally, the direct electron transfer between pAP and the electrode can be observed from the electrochemical cyclic voltammetry response, and it can be used to prepare electrochemical sensing devices [39].

The cyclic voltammograms (CV) of the four different electrodes are showed in Fig. 3.

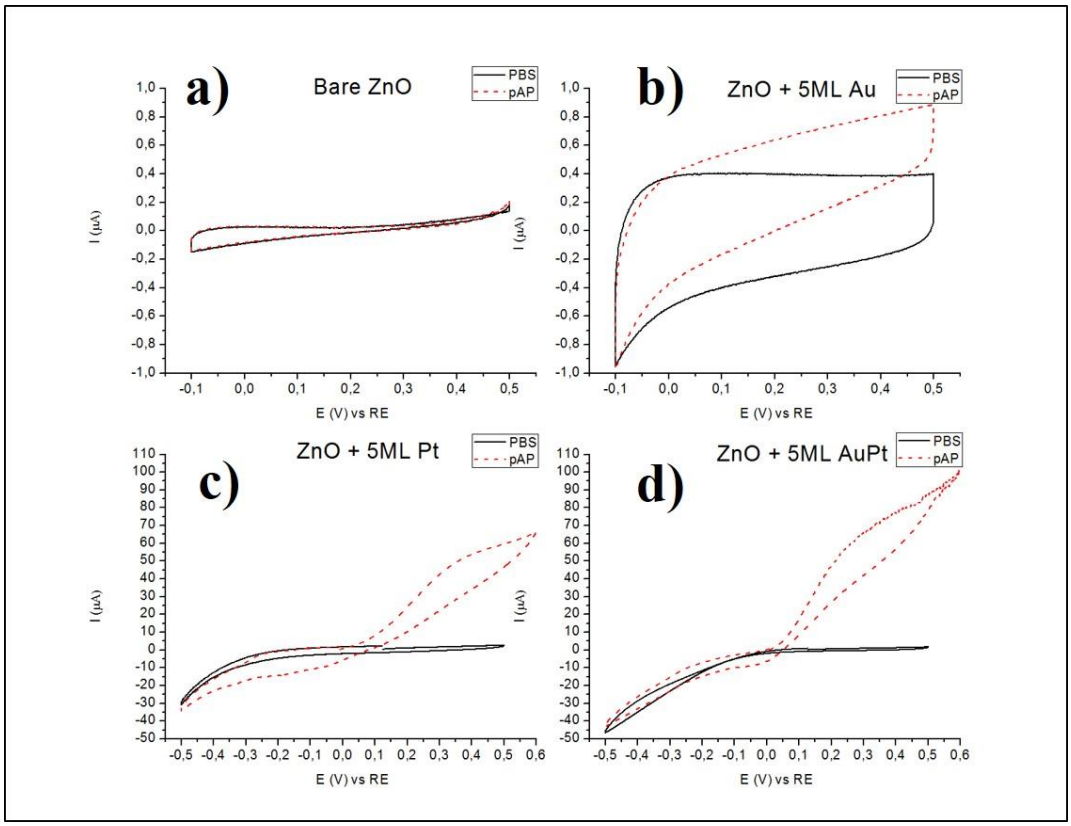

Fig. 3 – Cyclic voltammograms recorded in 0.1 M PBS (solid line) and in presence of 0.0916mM of pAP (dashed line) at different electrodes: (a) bare ZnO; (b) Au/ZnO; (c) Pt/ZnO; (d) AuPt/ZnO. Scan rate 50mV/s. Note the enlarged Y scale in top panels.

It can be seen that no response is detected with the unmodified ZnO electrodes (Fig. 3a), demonstrating that pAP cannot electrochemically react with the electrode. The situation slightly improves with the modification of the ZnO through the deposition of 5ML of Au

clusters. Despite the current response is low ~±0.8 μA; note that the signal is detectable and a small increase of the oxidation current with respect to the bare ZnO is achieved.

As observed in the case of the EIS analysis, the situation dramatically changes for Pt. The Pt/ZnO electrode shows a significant increase of the current response and a current peak at around 0.35 V, due to pAP oxidation. Thereofore, Pt clusters act as a catalyst towards the electro-chemical sensing of pAP by ZnO nanorods electrodes. Very interesting, the introduction of Au into Pt clusters further increases the current response of pAP at the same voltage. The measured current of AuPt/ZnO at 300 mV range increases by more than an order of magnitude compare to ZnO and Au/ZnO electrode. This increase indicates a very significant improvement of the catalytic abilities, making the Pt and AuPt nanocluster modified ZnO electrode suitable for chronoamperometry based electrochemical biosensors.

3.4 Chronoamperometry

Based on the cyclic voltammetry detection (Fig.3), the performance of Pt/ZnO and AuPt/ZnO clusters modified electrodes as detectors for pAP have been evaluated by amperometric experiments carried out at 0.375V vs. Ag/AgCl quasi-reference electrode.

Fig. 4 shows the amperometric responses of the two different electrodes to stepwise change of 0.01 mg/ml (0.0916 mM) pAP in 0.1 M PBS solution.

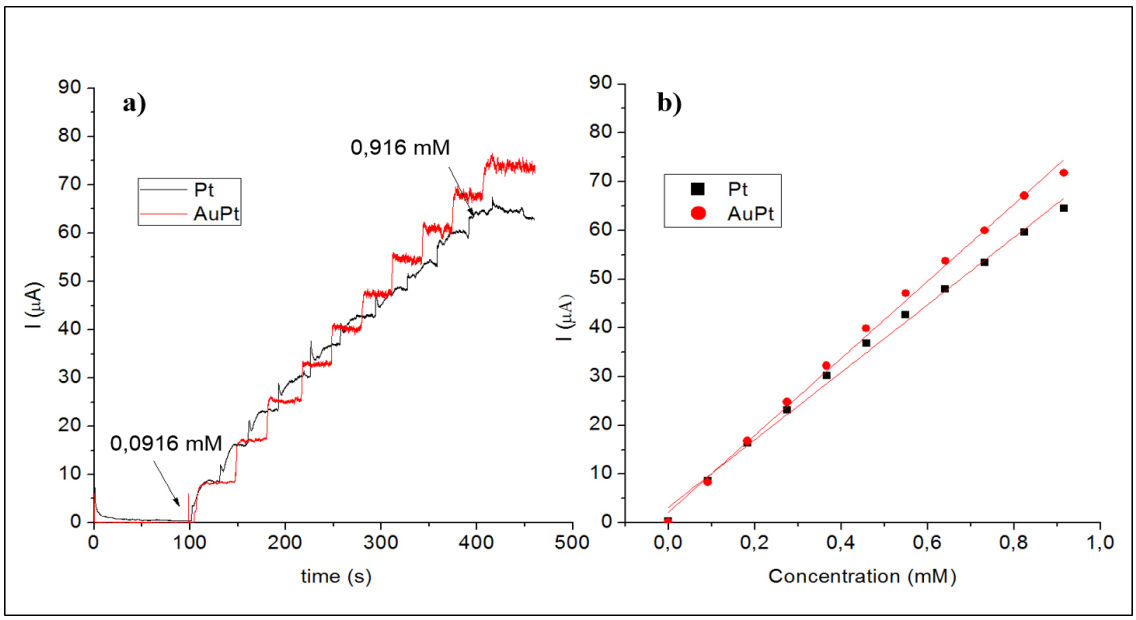

Fig. 4 – (a) Amperometric response of Pt/ZnO electrode (black line) and AuPt/ZnO electrode (red line) upon successive addition of 0.1mg/ml of pAP (0.0916mM) diluted in PBS 0.1 M at 0.375V vs. Ag/AgCl. (b) Calibration curve for the corresponding amperometric responses of pAP.

Both sensors show a good linear response (R^2 = 0.9939 for Pt/ZnO, R^2 = 0.996 for AuPt/ZnO), with bimetallic clusters modified electrode (AuPt/ZnO) exhibiting higher current than the single metal one, at the same applied voltage.

More specifically, the bimetallic system enhances the sensitivity and reduces the calculated 3-sigma-limit of detection compared to the Pt catalyst, as shown in Table 1. The signal from the bimetallic system electrode shows faster settling time, lower background noise and more flat steady state value compared to the Pt one. Additionally the bimetallic electrode has a slightly better minimum detectable signal (MDS) as compared to Pt only. This effect is probably due to the higher overpotential of the single particle system with respect to the

bimetallic system. The presence of Au in the alloy contribute to decrease the overpotential and enhance the oxidization current, as demonstrated in previous studies [44, 45].

Table 1 additionally summarizes the performance of various kinds of amperometric sensors for pAP detection reported by other researchers. Different types of electrodes were used for pAP sensor fabrication. Neto et al. prepared a glassy carbon electrode modified with hemin-based molecularly imprinted polymer with a sensitivity of 5.5 nA L μmol^{-1} [46]. Shiroma et al. produced a microfluidic gold and paper-based device that gave a LOD of 10.0 µmol L^{-1} [47]. The higher sensitivity of our system with respect to the one in [46] can be ascribed to the well-known catalytic properties of the Pt nanoparticles for the oxidation of many organic molecules [48-50]. Moreover, the lower LOD with respect to the electrode developed by Shiroma et al. is probably due to the use of bimetallic AuPt alloy clusters , which exhibits better electron transport that differ massively from the individual Au nanoparticles [51,52].

Ref.	**Electrode**	**Applied Voltage**	**Sensitivity [µA/mM cm^2]**	**LOD (3Sigma) [µM]**
This Work	Pt/ZnO	0.375 vs. Ag/AgCl	12.55	4.11
This Work	AuPt/ZnO	0.375 vs. Ag/AgCl	14.31	3.60
[43]	Carbon+Hemin based MIP	-0.1 vs. Ag/AgCl	5.50	3.0
[44]	Au on paper	0.4 vs. Au	-	10.0

Table 1 - Sensing performance towards the detection of pAP of different kinds of electrodes reported in literature.

4. Conclusions

We demonstrated how the performances of ZnO nanorods based electrode can be greatly improved through decoration with metal nanocluster. In the search of better electrodes, the electrochemical properties of ZnO nanorods decorated with Au, Pt and AuPt nanoclusters have been investigated. The results demonstrated the feasibility of Pt and AuPt modified ZnO

nanorods in detecting low concentrations of pAP; a typical product in many enzymatic biosensors. Electrodes of ZnO nanorods modified with metallic clusters have been produced, by using chemical bath deposition followed by laser ablation cluster beam deposition. Nearly mono-dispersed clusters were deposited in small amount, i.e. equivalent thickness of 5ML of clusters, and were obtained with uniform shape and distribution, covering the semiconductor. According to the electrochemical measurements, they were able to improve the electrochemical performance of the ZnO nanorods toward the sensing of pAP molecule.

In particular the bimetallic AuPt clusters exhibited an enhanced sensitivity of 14.31 μA/mM cm^2 and a limit of detection of 3.6 μM.

These results suggest that the catalytic properties of this material are very promising to detect specific electroactive products such as pAP. In the future such electrodes should be tested for other products, also in cases where the products are reduced such as in the case of H_2O_2.

5. Acknowledgements

The research leading to these results has received funding from the European Union's Seventh Framework Programme (FP7/2007-2013) under grant agreement n° 607417 (Catsense).

The authors thank Dr. Antonio Ferraro (IMM-Rome) for providing the ITO substrates.

References

[1] D. Aronoff and E. Neilson, The American journal of medicine 111.4 (2001): 304-315.

[2] T. Nemeth, P. Jankovics, et al., J. Pharm. Biomed. Anal. 47 (2008) 746–749.

[3] The European Pharmacopeial Convention, The European Pharmacopoeia, 6th edn, 2007, p. 49.

[4] The United States Pharmacopeial Convention, The United States Pharmacopoeia 27-NF (The National Formulary), 2004, p. 2494.

[5] Editor Committee of National Pharmacopoeia, Chinese Encyclopedia of Medicines, 2, Chemical Industry Press, Beijing, 2000, p. 206.

[6] H. Filik, et al., Sensors and Actuators B: Chemical 136 (2009), 105.

[7] B. Dejaegher et al., Talanta 75 (2008), 258.

[8] R. Wang et al., Electrochimica Acta 121 (2014), 102.

[9] N. G. Karousos., and M. R. Subrayal, Analyst 127 (2002), 368.

[10] Y. Fan, et al., Sensors and Actuators B: Chemical 157 (2011), 669.

[11] M. Jamal et al., Sensors and Actuators B 97 (2004), 59.

[12] Scandurra et al., Sensors 14 (2014), 8926.

[13] Chandrashekar, et al., Anal. Bioanal. Electrochem., 3 (2011), 224.

[14] P. Arora, A. Sindhu, N. Dilbaghi, and A. Chaudhury, Biosensors and Bioelectronics, 28 (2011), 1.

[15] A. Chaubey and B. Malhotra, Biosensors and bioelectronics, 17 (2002), 441

[16] W. R. Vandaveer, et al., Electrophoresis, 23 (2002), 3667.

[17] A. Janotti and C. G. Van de Walle, Reports on Progress in Physics, 72 (2009), 126501.

[18] Z. Dai, G. Shao, J. Hong, J. Bao, and J. Shen, 24, (2009), 1286.

[19] T. Kong, Y. Chen, Y. Ye, K. Zhang, Z. Wang, and X. Wang, Sensors and Actuators B: Chemical, 138 (2009) 344.

[20] J. Wang, X. W. Sun, A. Wei, Y. Lei, X. Cai, C. M. Li, and Z. L. Dong, Applied Physics Letters, (2006), 233106.

[21] J. Jung and S. Lim, Applied Surface Science, 265 (2013), 24.

[22] J. Zhao, D. Wu, and J. Zhi, Bioelectrochemistry, 75 (2009), 44.

[23] X. Liu, P. Lin, X. Yan, Z. Kang, Y. Zhao, Y. Lei, C. Li, H. Du, and Y. Zhang, Sensors and Actuators B: Chemical, 176 (2013) 22.

[24] V. Strano, R. G. Urso, M. Scuderi, K. O. Iwu, F. Simone, E. Ciliberto, C. Spinella, and S. Mirabella, The Journal of Physical Chemistry C, 118 (2014), 28189.

[25] M. Pea. L. Maiolo, R Pilloton, A Rinaldi, Rodolfo Araneo, E Giovine, A Orsini, A. Notargiacomo, Microelectronic Engineering 121, 147-152 (2014)

[26] X.L. Luo, A. Morrin, A.J Killard, M. R. Smyth, Electroanalysis, 18 (2006), 319.

[27] O.V. Salata, Journal of Nanobiotechnology, (2004), 1477.

[28] W. Bouwen et al., Rev. Sci. Instrum., 71 (2000) 54.

[29] M. C. Daniel and D. Astruc, Chem. Rev., 104 (2004), 293.

[30] S. Zeng, et al. Plasmonics, 6.3 (2011), 491.

[31] K. Saha, et al., Chemical reviews, 112 (2012), 2739.

[32] Y. Chen, et al., Journal of Materials Chemistry, 21 (2011), 7604.

[33] Polsky, Ronen, et al., Analytical Chemistry, 78 (2006), 2268.

[34] Y. Li, Yongjie, et al., Carbon, 48 (2010), 1124.

[35] L.Q. Rong, et al., Talanta, (2007), 819.

[36] T. Han, et al., Sensors and Actuators B: Chemical, 207 (2015), 404.

[37] F. Xiao, et al., Biosensors and Bioelectronics, 24 (2009), 3481.

[38] M. Yuan, et al., Sensors and Actuators B: Chemical, 190 (2014), 707.

[39] T. Yoetz-Kopelman, et al., Sensors and Actuators B: Chemical, (2016).

[40] B.Y. Chang and S.M. Park, Annual Review of Analytical Chemistry, 3 (2010): 207.

[41] J. E. B. Randles, Discussions of the Faraday Society, 1 (1947), 11.

[42] V. Subramanian et al., Journal of the American Chemical Society 126.15 (2004), 4943.

[43] K. Rajeshwar, Encyclopedia of electrochemistry (2007).

[44] Lin, Yuanyuan, et al., Microchimica Acta 175 (2011): 259.

[45] D.N. Oko, Daniel Nii. *"Electrocatalytic Activity of Small Organic Molecules at PtAu Alloy Nanoparticles for Fuel Cells and Electrochemical Biosensing Applications"*. Diss. Université Mcgill, 2014.

[46] J.R.M. Neto et al., Sens. And Act. B, 152 (2011) 220.

[47] L.Y. Shiroma et al., Analytica Chimica Acta, 725 (2012) 44.

[48] J. Greeley et al., Annual Review of Physical Chemistry 53.1 (2002): 319.

[49] N.M. Markovic et al., Electrochim. Acta, 40 (1995) 91.

[50] B. Beden et al. Journal of Electroanalytical Chemistry and Interfacial Electrochemistry 142 (1982): 171.

[51] J. Zhang, D. N. Oko, S. Garbarino, M. Chaker, A. C. Tavares, D. Guay, D. Ma, J. Phys. Chem. C (2012), 116 (24), 13413.

[52] D. Mott et al., Catalysis Today 122 (2007): 378.

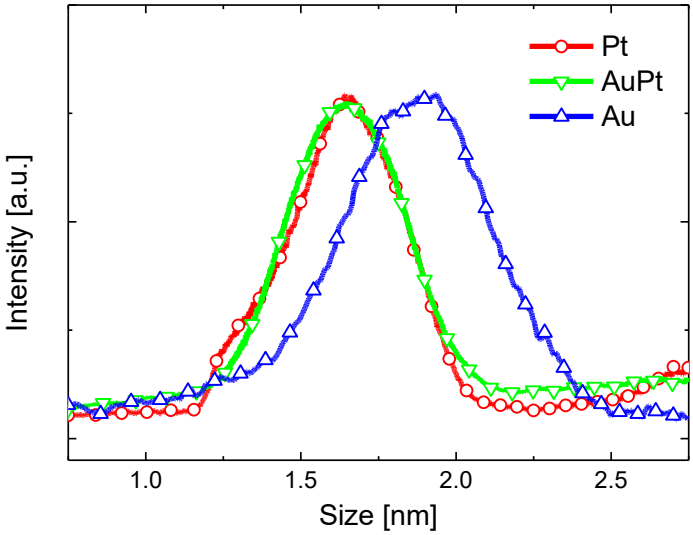

Supporting Information

Fig. S1 – Reflected Time Of Flight (RTOF) size distribution spectra of unselected size Au, AuPt and Pt clusters. Spectra were obtained by considering the RTOF (m/z) signal of cationic (single positive charged) clusters. The conversion of RTOF spectra from m/z distribution to cluster size distribution is based on the assumption of spherical clusters with size $d_{cluster} = 2\left(\frac{m/z}{m_{at}}\right)^{1/3} r_{at}$, where m_{at} is the atomic mass of the element in a.m.u and r_{at} the atomic radius.

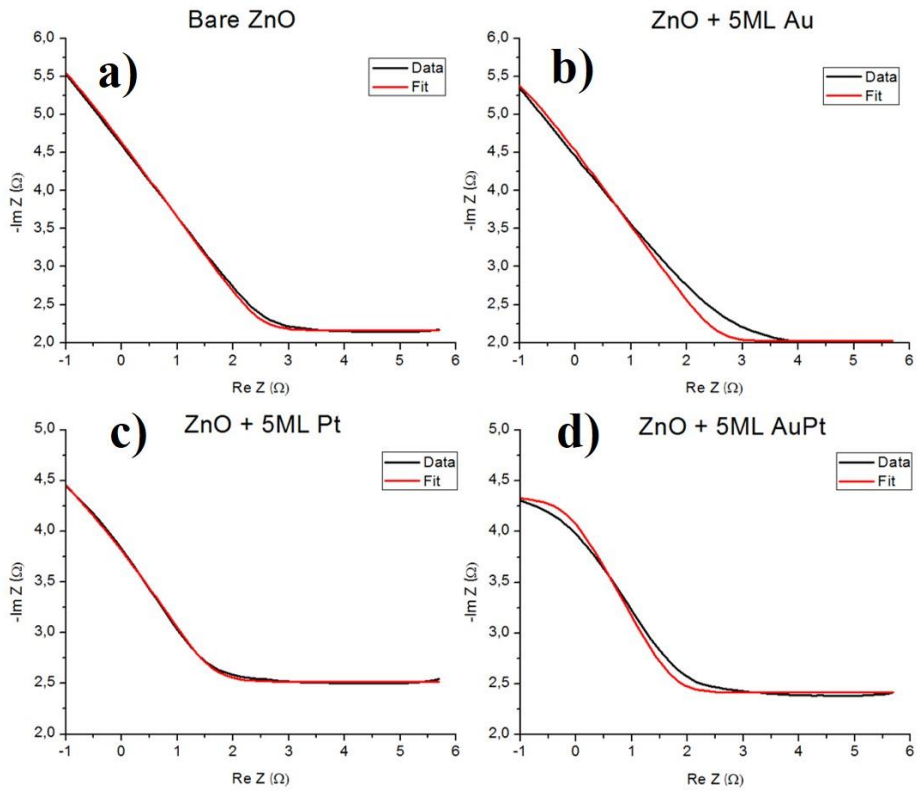

Fig. S2 – Bode plots showing the good agreement of the data and the fit calculated using the Randles model for the different kinds of electrodes.

Electrode	**Bare ZnO**	**Au/ZnO**	**Pt/ZnO**	**AuPt/ZnO**
R_s	145,7 Ω	105,3 Ω	336 Ω	259,1 Ω
R_{ct}	251,2 kΩ	199,6 kΩ	25,1 kΩ	19,9 kΩ
C_{dl}	3,52 µF	4,6 µF	20,0 µF	11,1 µF
A_w	$5{,}18 \times 10^5\ \Omega\ s^{-0.5}$	$2{,}04 \times 10^5\ \Omega\ s^{-0.5}$	$6{,}59 \times 10^3\ \Omega\ s^{-0.5}$	$1{,}16 \times 10^3\ \Omega\ s^{-0.5}$

Table S1 – Fitted impedance values obtained with the Randles model for the different kinds of electrodes.